

A phase-matchable nonlinear optical crystal 4-amino-5-mercapto-3-[1-(4-isobutylphenyl)ethyl]- 1,2,4-triazole: Synthesis, crystal growth and characterization

K NASEEMA¹, VIJAYALAKSHMI RAO^{1,*}, K V SUJITH²
and BALAKRISHNA KALLURAYA²

¹Department of Materials Science, Mangalore University, Mangalagangothri 574 199, India

²Department of Chemistry, Mangalore University, Mangalagangothri 574 199, India

*Corresponding author. E-mail: vijraobrns@rediffmail.com; vijrao@yahoo.com

MS received 10 December 2008; revised 6 May 2009; accepted 23 May 2009

Abstract. In this paper, we report the synthesis, growth and characterization of a new organic NLO single crystal of 4-amino-5-mercapto-3-[1-(4-isobutylphenyl)ethyl]-1,2,4-triazole (AMIT). The title compound is synthesized and single crystals were grown by the slow evaporation technique at room temperature. The grown crystal was characterized by powder XRD, FTIR, UV–Vis. and microhardness studies. The thermal analysis of the crystal was carried out by TGA, DTA and DSC. From DSC, the melting point of the crystal is found to be 168°C. The scanning electron microscopy (SEM) provides information about the surface morphology of the crystal. The SHG efficiency has been estimated as 0.3 times that of KDP using Kurtz powder method and is found to be a phase-matchable NLO crystal.

Keywords. Non-linear optical crystal; growth from solution; characterization; organic material.

PACS Nos 42.70.Mp; 42.65.k; 42.65.ky; 42.79.Nv

1. Introduction

Extensive studies have been made on the synthesis and crystal growth of nonlinear optical (NLO) materials over the past decade because of their potential application in the field of telecommunication, optical signal processing and optical switching. Organic materials have been of particular interest because the NLO responses in this broad class of materials are microscopic in origin, offering an opportunity to use theoretical modelling coupled with synthetic flexibility to design and produce novel materials [1,2]. By converting the IR laser radiation into useful visible–UV wavelength and in particular with the generation of the blue–violet via second-order nonlinear optical (SONLO) material, several applications such as high density data

storage, laser printing, displays, inflorescence, photolithography, remote sensing, chemical and biological species detection, high resolution spectroscopy, medical diagnosis, underwater monitoring and communication can be realized [3]. Considerable theoretical and experimental investigations have been done in order to understand the microscopic origin of nonlinear behaviours of organic NLO materials [4,5]. Organic molecules with significant nonlinear optical activity generally consist of a π -electron conjugated moiety substituted by an electron donor group on the other end, forming a push-pull conjugated structure. The conjugated π -electron moiety provides a pathway for the entire length of conjugation under the perturbation of an external electric field. Functionalization of both ends of the π bond system with appropriate electron donor and acceptor group can increase the asymmetric electronic distribution in either or both the ground and excited states, thus leading to an increased optical nonlinearity [6].

For efficient second harmonic generation (SHG), one requires highly polarizable molecular system having asymmetric charge distribution in the molecule, that is substituted donor and acceptor groups at the end of the molecule with noncentrosymmetric crystal structure [7]. The molecular structure of the grown crystal contains both amino and methyl groups. The methyl group is an electron donor and the amino group is an electron acceptor.

2. Experimental

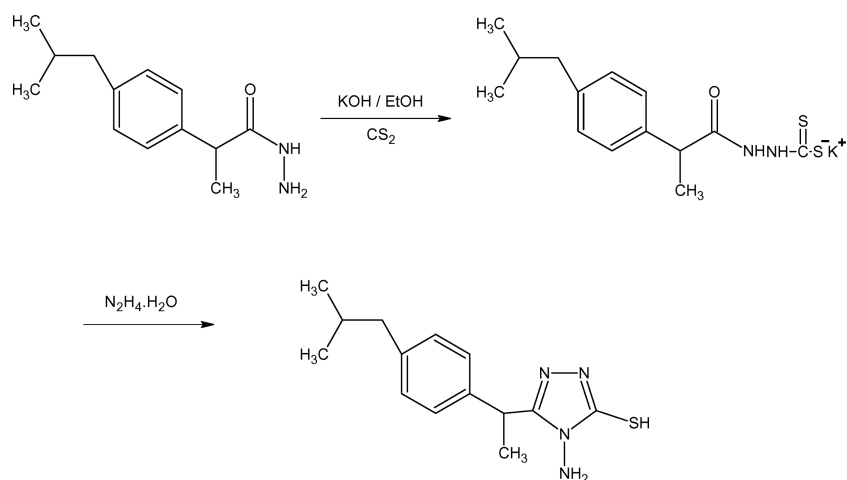
2.1 Material synthesis

Hydrazide, the starting compound, was obtained by the hydrazinolysis of the corresponding ester with hydrazine hydrate in ethanol. The hydrazide thus obtained was converted to its potassium dithiocarbazinate by stirring with carbon disulphide in alcoholic KOH. The obtained mixture of potassium dithiocarbazinate, hydrazine hydrate and water was gently heated so that it starts boiling. Heating was continued until the evolution of hydrogen sulphide was ceased. The reaction mixture was cooled to room temperature and diluted with water. It is then acidified with dil. HCl. The solid mass separated was collected by filtration, washed with water and dried to get the final compound 4-amino-5-mercapto-3-[1-(4-isobutylphenyl)ethyl]-1,2,4-triazole. Recrystallization was done to purify the synthesized compound (scheme 1).

2.2 Crystal growth

Single crystals of 4-amino-5-mercapto-3-[1-(4-isobutylphenyl)ethyl]-1,2,4-triazole were grown from ethanol by slow evaporation of the solvent at room temperature. Saturated solution of the compound in ethanol was taken in a conical flask and was kept at room temperature. After a growth period of five days, due to slow evaporation of the solvent, optically transparent crystals of about $5 \times 4 \times 3 \text{ mm}^3$ dimension were harvested and are shown in figure 1.

(4-Amino-5-mercapto-3-[1-(4-isobutylphenyl)ethyl]-1,2,4-triazole



Scheme 1.

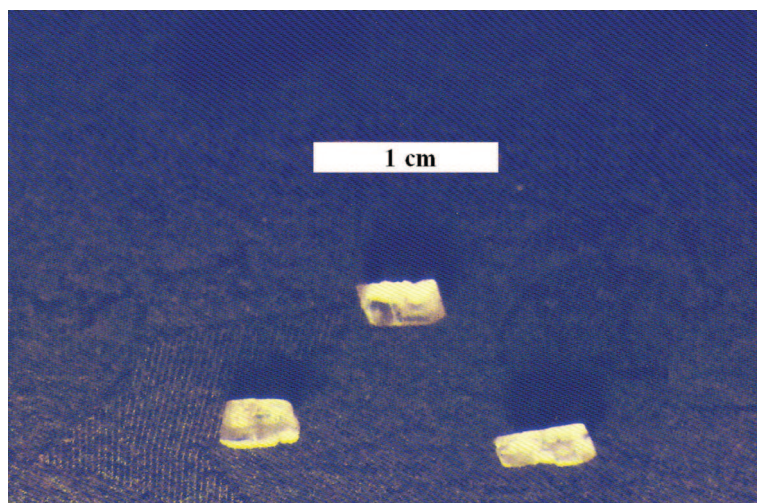


Figure 1. Photograph of the grown AMIT crystal.

3. Characterization

3.1 UV-visible spectroscopy

UV-visible spectrum of the grown crystal was recorded using a SHIMADZU UV-VIS-NIR scanning spectrophotometer, model 3101 PC. There is no absorption of light from near UV to the near IR (figure 2). Absorption spectrum of the NLO material plays a major role in device fabrication. Wider the transparency window, more will be the practical applicability of the material. Optical absorption spectrum of the grown crystal was recorded in the wave range of

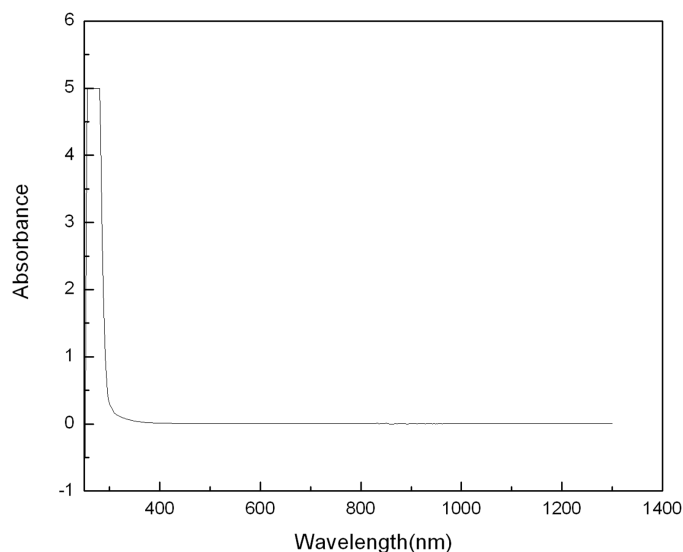


Figure 2. UV spectrum of AMIT.

200–1300 nm. The lower cut off is observed at 300 nm. The absorption is negligible in the entire visible region of the electromagnetic spectrum. Therefore, it can be used as a potential material for SHG in the visible region.

3.2 FTIR spectroscopy

The FTIR spectrum of the grown crystal was recorded in the KBr phase within the frequency region $400\text{--}4000\text{ cm}^{-1}$, using SHIMADZU 8400S FTIR spectrometer (figure 3). In the FTIR spectrum of the studied compound, the peak due to aromatic C–H stretching appeared as an absorption band at 3141 cm^{-1} . The bands around $1379\text{--}1497\text{ cm}^{-1}$ correspond to the frequency of the bending vibrations of C–H bonds. The N–H stretching absorption was observed at around 3321 cm^{-1} . The C=N stretching frequency at 1568 cm^{-1} and C=S stretching frequency at 1103 cm^{-1} were observed.

3.3 XRD studies

The XRD pattern of the powdered crystal is recorded in a BRUKER AXS-D 8 Advance with copper target ($\lambda = 1.54\text{ \AA}$) (figure 4). The revelation of the well-defined Bragg reflections at specific 2θ angles in the diffraction patterns suggests crystallinity of the sample. The hkl and d values are given in table 1.

(4-Amino-5-mercapto-3-[1-(4-isobutylphenyl)ethyl]-1,2,4-triazole

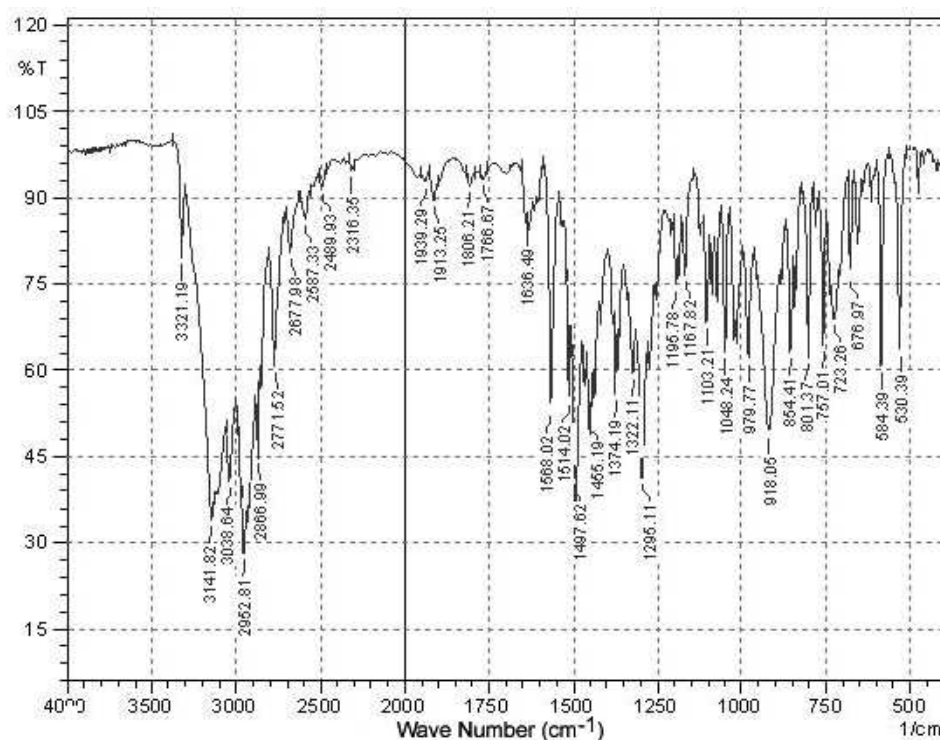


Figure 3. FTIR spectrum of AMIT.

Table 1. XRD data of AMIT.

| h | k | l | m | d (Å) | Peak position (2θ) |
|-----|-----|-----|-----|---------|-----------------------------|
| 1 | 0 | 2 | 2 | 4.31786 | 20.55292 |
| 0 | 0 | 4 | 2 | 3.71031 | 23.96468 |
| 1 | 2 | 0 | 4 | 3.43455 | 25.92098 |
| -1 | 0 | 4 | 2 | 3.36018 | 26.50503 |
| 1 | 2 | 2 | 4 | 3.02268 | 29.52817 |
| 0 | 3 | 1 | 4 | 2.77222 | 32.26545 |
| 1 | -2 | -5 | 4 | 2.34414 | 38.36828 |
| -3 | 0 | 1 | 2 | 1.97872 | 45.82072 |
| 1 | 5 | 0 | 4 | 1.62694 | 56.51870 |

3.4 SHG measurement

The absence of absorption in the entire visible region makes the crystal a potential candidate material for second harmonic generation in the visible region, especially in blue-violet and near infrared region. Nonlinear optical property of the crystal was

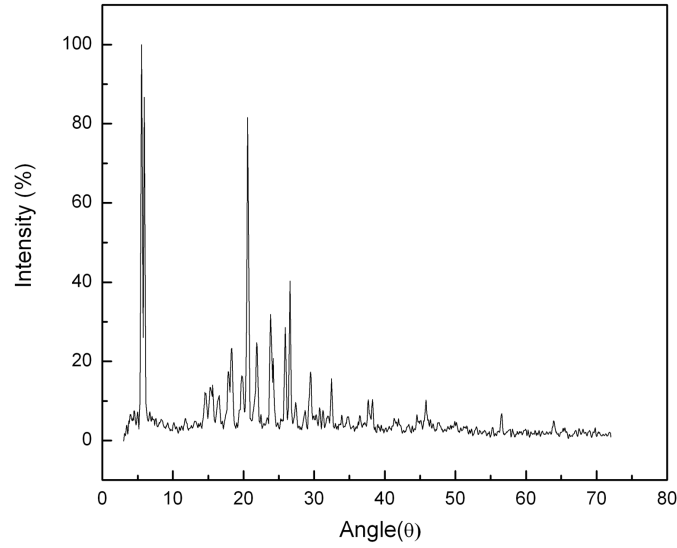


Figure 4. Powder XRD pattern of AMIT.

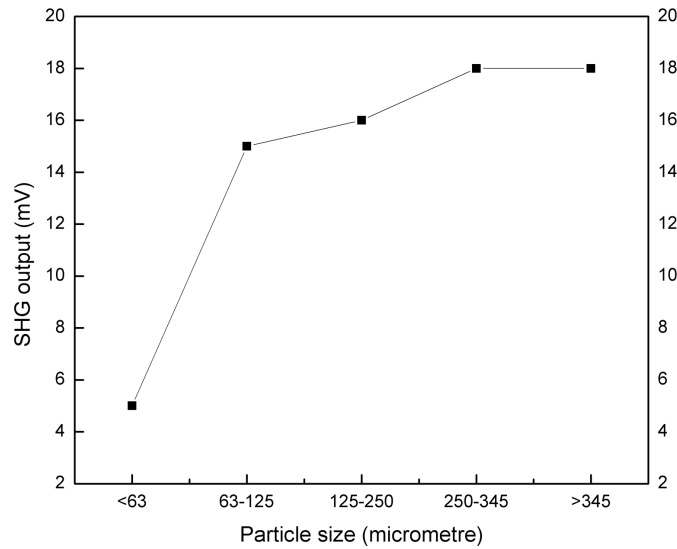


Figure 5. Variation of SHG with the particle size for AMIT.

found using Kurtz and Perry powder SHG technique by passing the fundamental beam of Q-switched, mode locked Nd:Yag laser operating at $1.06\ \mu\text{m}$ and generating pulses of 8 ns and energy 2.2 mJ/pulse. The emission of green radiation confirms the NLO property of the sample and it is 0.3 times that of KDP.

(4-Amino-5-mercapto-3-[1-(4-isobutylphenyl)ethyl]-1,2,4-triazole

To confirm the existence of phase-matching direction in the crystal, the particle size dependency was studied. Particles of size ranging from <63, 63–125, 125–250, 250–345 and >345 μm were obtained using standard sieves of 63, 125, 250 and 345 μm . The SHG intensity increases with the increase in particle size from <63 to 125 μm (5–15 mV). Above this range, the SHG intensity becomes almost independent of particle size (15–18 mV) (figure 5). This kind of particle size dependency on SHG intensity exists only in phase-matchable materials. Hence this crystal can be used as an efficient frequency doubler and optical parametric oscillator provided large size single crystals are available.

3.5 Thermal analysis (TG/DT and DSC)

The TGA curve gives useful information regarding the thermal stability and composition of the sample under investigation. The recorded thermogram is first analysed for obtaining the percentage weight loss at different temperatures and hence about the thermal stability and dissociation of the crystal. Thermogravimetric run was taken on Perkin Elmer Diamond TG analyser by scanning at the rate of 10 K/min in an atmosphere of nitrogen, in the temperature range 40–650°C (figure 6). The initial mass of the material subjected to analysis was 5.524 mg and the final mass left out after the experiment was only 18% of the initial mass at a temperature of about 650°C, indicating the bulk decomposition occurring in the sample. From the curves, it is inferred that the vapourization takes place in the vicinity of 306°C. Gradual and significant weight loss was observed as the temperature increases. Also it is seen that, an almost total decomposition of the compound takes place at a temperature of about 650°C. Since the decomposition temperature is beyond 100°C, there is no evidence for entrapped water in the crystal lattice or any adsorbed water on the crystal surface. The DSC analysis was done between 30 and 200°C at a heating rate of 10°C/min in the nitrogen atmosphere and is shown in figure 7. From the peak it is inferred that the melting of the material takes place at 168°C.

3.6 Microhardness measurement

The mechanical property plays a vital role in device fabrication. In the present work, the Knoop hardness indentations were carried out on the grown crystal for the applied load of 1, 3, 5, 10 and 25 g and table 2 shows the hardness number and the diagonal length for various loads. The indentation time was kept as 10 s for each load. Microcracks were observed in the sample due to the mechanical stress when a load of 50 g was added. It is observed that the hardness number first increases and then decreases with increasing load. The long diagonal length was used in calculating the Knoop hardness number using the formula $H = 14228.8 \times P/d^2$, where P is the applied load in g and d is the mean diagonal length in microns. The indentation time of 10 s was kept constant, as this time was adequate to minimize the vibration effect on the result.

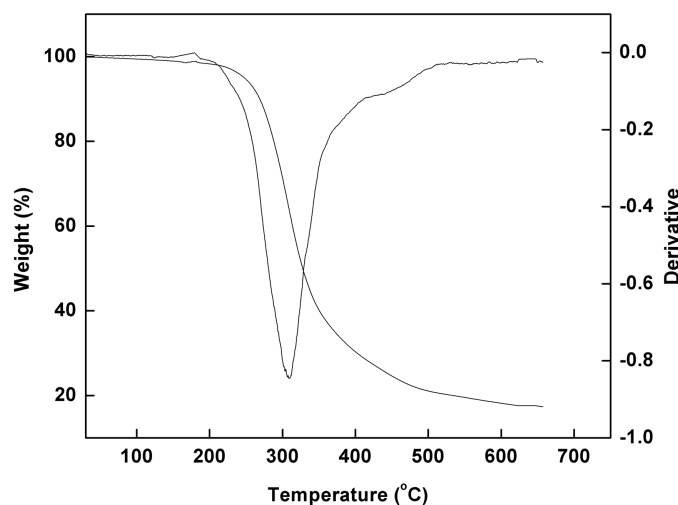


Figure 6. TG/DT curve of AMIT.

Table 2. The hardness number and the diagonal length for various loads.

| Load (g) | Knoop hardness (kg/mm ²) | Diagonal length (μ m) |
|-------------|---|-------------------------------|
| 1 | 8 | 41.9 |
| 3 | 25 | 5.3 |
| 5 | 62 | 33.8 |
| 10 | 12 | 107 |
| 25 | 91 | 195.8 |

There are a few papers on the pyramidal hardness of some organic and inorganic molecular solids [8,9]. In all these studies, one observes that the load variation was studied using the standard set of weights available in the weight box. Some detailed studies were done using weights having small differences [10–12]. These studies showed that the plots of hardness variation with load was not just a curve which increased or decreased at low load and then remained steady, but exhibited two and sometimes three peaks. These peaks are due to the slip taking place in different planes and directions.

The hardness of a material depends on its plastic and elastic properties. In the case of Knoop indentations, the elastic recovery takes place along the short diagonal only and the long diagonal does not change when the load is removed. When a loaded indenter penetrates a solid, the depth of penetration increases until the condition of lattice immediately below the indenter has the same characteristics as that of the specimen in which the saturation value of the compressive strain has been attained. The strain becomes progressively smaller with increasing distance

(4-Amino-5-mercapto-3-[1-(4-isobutylphenyl)ethyl]-1,2,4-triazole

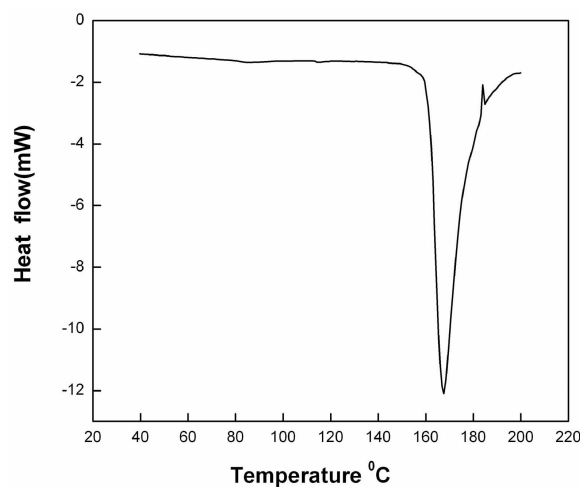


Figure 7. DSC curve of AMIT.

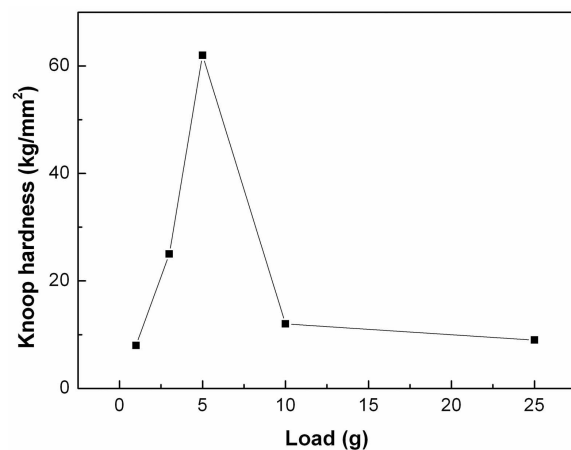


Figure 8. Load vs. hardness of AMIT.

from the centre of the material to a distance equal to the length of the long diagonal. The grown crystal shows a peak in the plot of hardness vs. load (figure 8), having a hardness number of 62 kg/mm² at a load of 5 g. This peak corresponds to the slip taking place on different planes and directions.

3.7 SEM studies

Figure 9 shows the SEM micrographs of the grown crystal corresponding to different magnifications. The surface morphology of the epilayers was found to have microcrystallites/clusters on the sample.

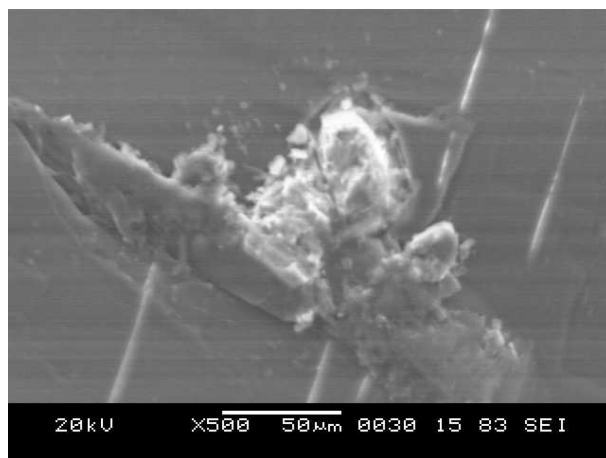


Figure 9. SEM photograph of AMIT.

4. Conclusion

Single crystals of 4-amino-5-mercapto-3-[1-(4-isobutylphenyl)ethyl]-1,2,4-triazole were grown from ethanol by slow evaporation of the solvent at room temperature. Powder XRD confirms the crystallinity of the sample. Vibrational frequencies were assigned from FTIR spectral analysis which confirms the presence of functional groups. Optical absorption studies show that the sample is optically transparent over a wide wavelength region and minimum absorption is observed in the entire visible region. TGA/DSC shows good thermal stability of the material. Its SHG efficiency is found to be 0.3 time that of KDP. Knoop hardness test shows that the crystal is stable up to 25 g.

Acknowledgement

The authors are grateful to Prof. P K Das, IISc, Bangalore for extending the facilities to measure SHG efficiency.

References

- [1] P N Prasad and D J Williams, *Introduction to nonlinear optical effects in organic molecules and polymers* (Wiley, New York, 1991)
- [2] D S Chemla and J Zyss, *Nonlinear optical properties of organic molecules and crystals* (Academic Press, New York, 1987)
- [3] Guanghus Zhang, Mingguo Lin, Dong Xu and Duorong Yuan, *J. Mater. Sci. Lett.* **19**, 1255 (2000)
- [4] Y Iitaka, *Acta Crystallogr.* **14**, 1 (1961)
Full text Via Cross Ref/View Record in Scopus/Cited by in Scopus (z)
- [5] R Christian, *Solvents and solvent effects in organic chemistry* (VCH, New York, 1990)

(4-Amino-5-mercapto-3-[1-(4-isobutylphenyl)ethyl]-1,2,4-triazole

- [6] H Ringertz, *Acta Crystallogr.* **B27**, 285 (1971)
- [7] R W Munn and C N Ironside, *Principles and applications of nonlinear optical materials* (Chapman and Hall, London, 1993)
- [8] E M Hampton, R M Hooper, B S Shah and J N Sherwood, *Philos. Mag.* **29**, 743 (1974)
- [9] P J Helpenny, K J Roberts and J N Sherwood, *J. Mater. Sci.* **19**, 1689 (1984)
- [10] R K Marwaha and B S Shah, *Cryst. Res. Technol.* **23**, K63 (1988)
- [11] R K Marwaha and B S Shah, *Cryst. Res. Technol.* **26**, 491 (1991)
- [12] R K Marwaha and B S Shah, *Cryst. Res. Technol.* **27**, 1097 (1992)